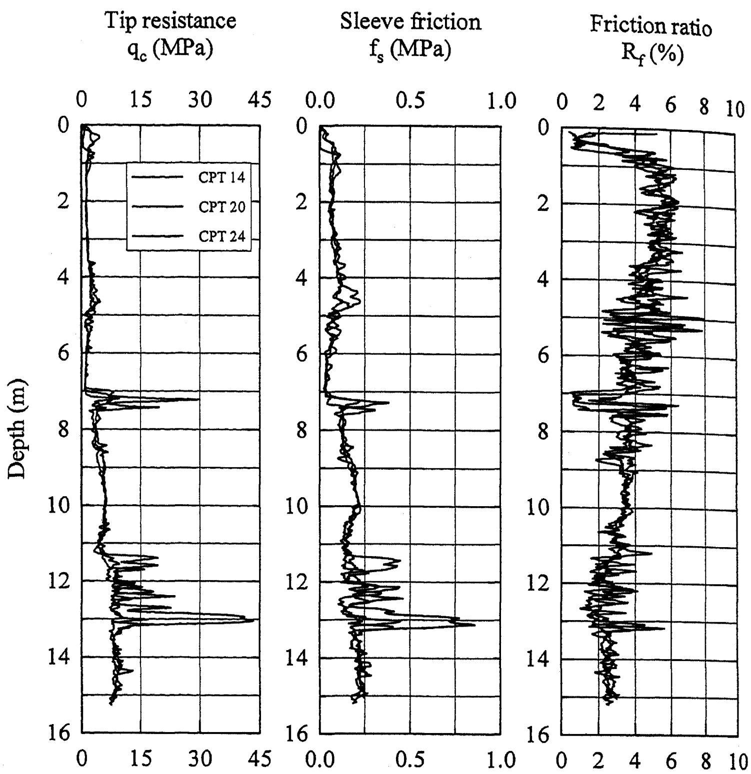

Figure 5: CPT soundings using the standard 10-cm^2 cone penetrometer at NGES-TAMU clay site.

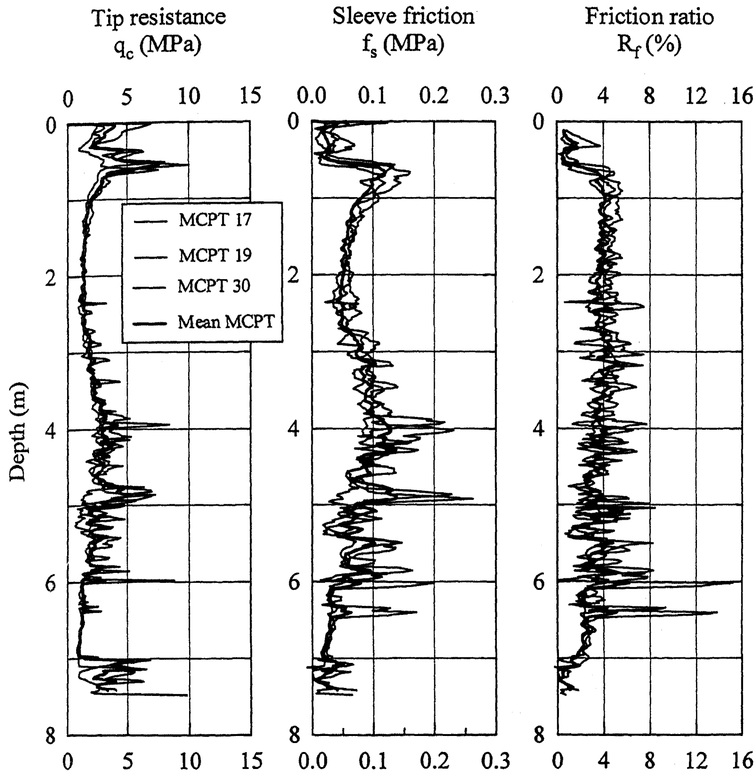

Figure 6: Miniature cone penetration tests at the NGES-TAMU clay site.

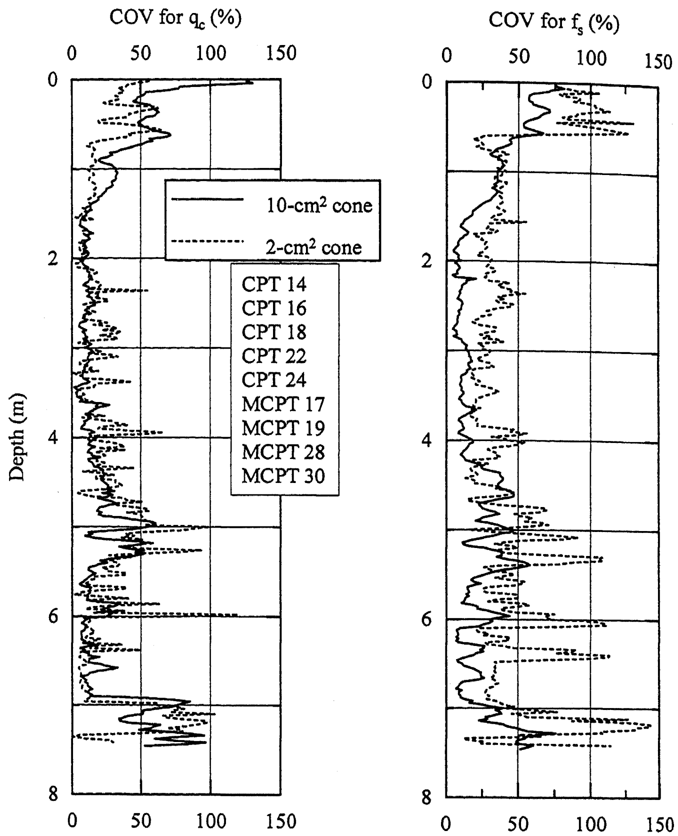

Figure 7: Analysis of repeatability of the CPT and MCPT tests at the NGES-TAMU clay site.

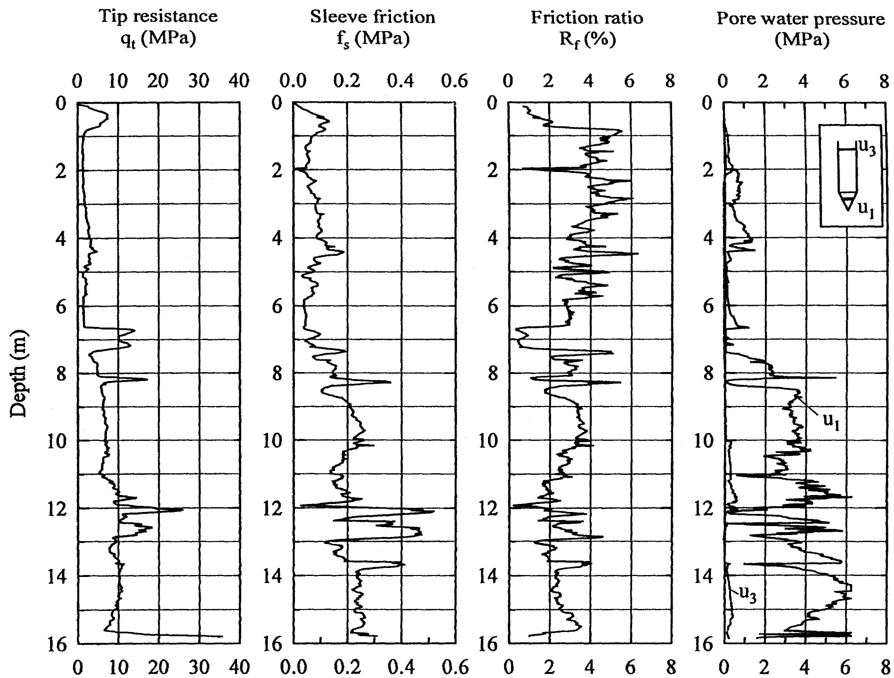

Figure 8: Piezocone penetration test (15-cm^2) at the NGES-TAMU clay site.

Soil Profile and Properties from CPT

The CPT test results of the standard cone were used to identify the soil profile using soil classification and identification methods by Robertson et al. (1986), Olsen and Mitchell (1995), Zhang and Tumay (1999). The latest method (Zhang and Tumay, 1999) considers the correlation between the composition and mechanical behavior of soils. The two major approaches in soil classification by Zhang and Tumay (1999) are the probabilistic region estimation and the fuzzy approach. The probabilistic region estimation is similar to conventional soil classification systems where it depends on soil composition. In this classification method, the probability of identifying the soil type is calculated. Soil types are divided into three soil categories: clayey, silty, and sandy soils. The CPT fuzzy classification system focuses on the soil behavior and defines three soil types: highly probable clayey soil (HPC), highly probable mixed soil (HPM), and highly probable sandy soil (HPS).

Estimated soil profiles using CPT soundings are compared with the particle size distribution profile in Figure 9. Considering the upper 7-m, all interpretation methods showed that clay is the predominant constituent of the soil. This is consistent with the particle size distribution and with the soil profile in Figure 3. The beginning of the sand channel is recognized at 7 m below the ground surface while its thickness varies depending on the method used to estimate the soil profile. Below the sand channel, the estimated soil profiles are combinations of clay, silt, and sand. Briaud (1997) reported the presence of fine-grained sand layers within the clay below the sand channel. Zhang and Tumay (1999) methods show soil profiles with probabilistic quantitative evaluation of the clay, silt, and sand. For example, the particle size analysis shows the amount of clay starts decreasing with depth at 9 m, while the silt and sand percentages are increasing. The probabilistic region estimation and fuzzy methods showed a similar trend, while the other interpretation methods showed a sudden jump from one soil layer to another. Considering the soil from 1 to 3.5 m deep, q_c (q_t) and f_s demonstrate that the layer is *homogenous*. Zhang and Tumay (1999) interpretation methods predicted a layer of clay, which is consistent with the *constant* values for q_c (q_t) and f_s (Figures 5-8) and with high percentage of clay at 3 m from particle size analysis.

The soil profile identified from the miniature cone output by the probabilistic region estimation approach (Zhang and Tumay, 1999) is shown in Figure 10. The miniature cone recognized finer soil details such as small layers and pockets/lenses of sand and silt within the clay deposit. The soil profile is compatible with those obtained from the CPT test data and the hydrometer analysis shown in Figure 9.

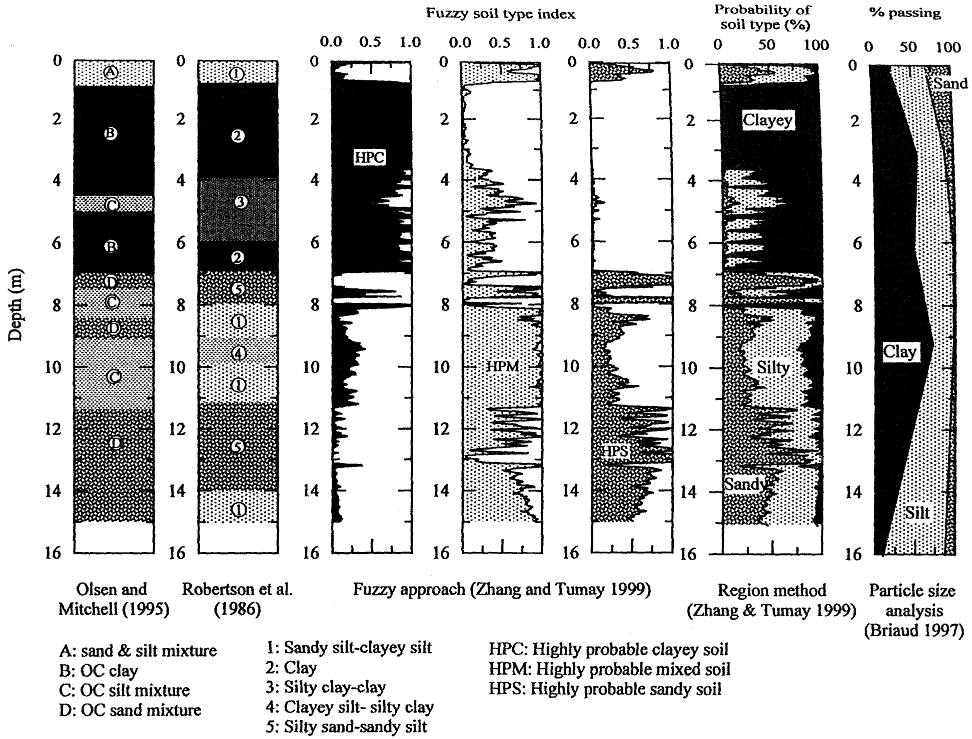

Figure 9: Comparison of different classification methods - average Standard CPT soundings at the NGES-TAMU clay site.

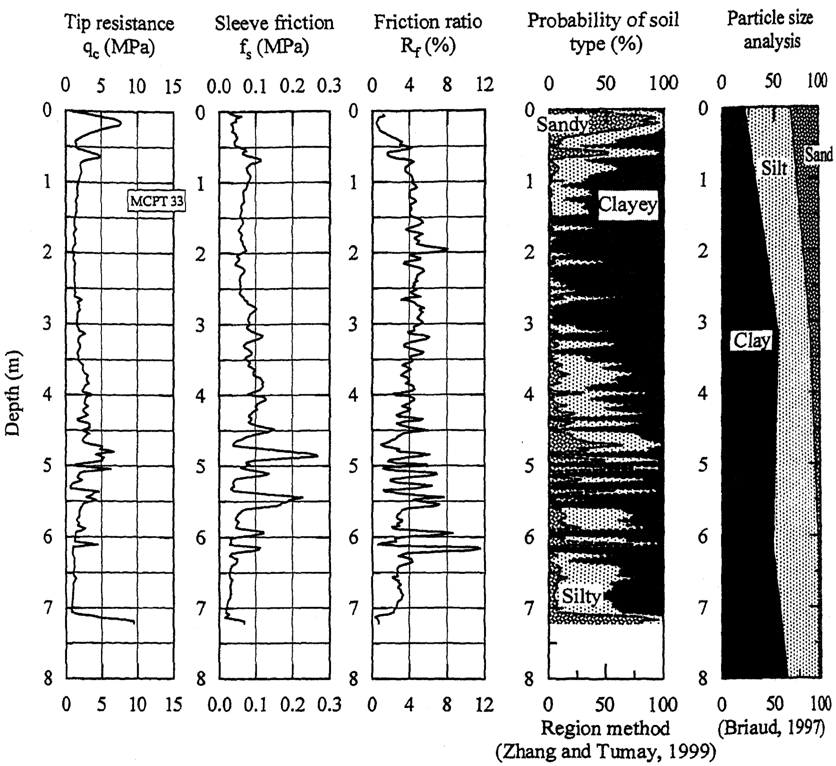

Figure 10: Estimated soil profile from miniature cone penetration test at the NGES-TAMU clay site.

Cone penetration tests were conducted using cones of different sizes and functions. However, the different soundings are consistent and reflect a similar pattern. A summary of cone penetration test results for the top stiff clay layer (0.6-5.5 m) is presented in Table 2. Considering this layer, the average cone tip resistance (q_c) is 2.05 MPa and the average sleeve friction (f_s) is 78 kPa. The average corrected tip resistance (q_t) is 2.4 MPa. Briaud (1997) described the top stiff clay layer as very uniform in thickness to about 5.5 m and reported the average cone tip resistance (q_c) is 2.0 MPa.

The undrained shear strength (s_u) can be estimated from the CPT test by:

$$s_u = \frac{q_c - \sigma_{vo}}{N_k} \tag{1}$$

where q_c is the total cone resistance, N_k is the empirical cone factor, and σ_{vo} is the total overburden pressure. Using s_u obtained from triaxial compression tests, Kjekstad et al. (1978) found the average N_k equals to 17 for non-fissured overconsolidated clay. This value (N_k=17) was assumed for this soil to estimate the undrained shear strength. Considering the clay layer from 0-5.5 m, s_u is 115 kPa as calculated from Equation 1 using the average values of q_c, and σ_{vo}. The undrained shear strength was also calculated using Equation 1 every 2 cm of soil depth, then the average undrained shear strength for the soil layer was obtained as s_u=109 kPa. The predicted undrained shear strength values are in agreement with the average s_u=110 kPa from UU triaxial tests (Briaud, 1997).

The overconsolidation ratio (OCR) can be estimated using the CPT by different methods. Lunne et al. (1997) described methods of estimating the OCR based on the undrained shear strength. The OCR values for this site were predicted following their procedure and using Andresen et al. (1979) correlation. The predicted OCR values with depth are compared with experimental results in Figure 11. This method underpredicted the OCR interpreted from experimental data for this site. The predicted OCR decreased with depth, which is consistent with the general trend. Briaud (1997) described the overconsolidation ratio for the top soil layer (0-5.5 m) as high and for the second layer (6.5-12.5 m) as moderate.

Chen and Mayne (1994) suggested the following simplified expression to estimate OCR from PCPT with u_1 measurement:

$$OCR = 0.81\frac{q_t - u_1}{\sigma'_{vo}} \tag{2}$$

The OCR profile with depth was also estimated using Equation 2. The results are compared with experimental data in Figure 11. Equation 2 overpredicted the OCR values especially for the very stiff clay layer (from 6.5-12.5 m). Equation 2 uses the pore pressure u_1 to predict the OCR. The very stiff clay layer has a very high cone tip resistance (average q_c is about 6 MPa), which is the reason for the predicted high OCR values.

TABLE 2– Analysis of CPT and MCPT soundings for the top stiff clay layer (depth from 0.6 to 5.5 m) at the NGES-TAMU clay site.

Test No.	Average Tip Resistance q_c (MPa)	Average Sleeve Friction f_s (kPa)	Average Friction Ratio R_f (%)	Test No.	Average Tip Resistance q_c (MPa)	Average Sleeve Friction f_s (kPa)	Average Friction Ratio R_f (%)
2-cm^2 miniature friction cone penetrometer				10-cm^2 friction cone penetrometer			
MCPT13	2.08	90.8	4.5	CPT14	1.91	94.2	5.1
MCPT17	2.36	91.3	4.2	CPT16	2.04	100.0	5.1
MCPT19	2.27	80.8	3.7	CPT18	1.93	95.5	5.4
MCPT21	2.24	77.3	3.7	CPT22	1.72	80.3	4.9
MCPT23	2.17	81.8	4.1	CPT24	1.83	86.4	4.9
MCPT27	2.26	80.5	3.9	15-cm^2 piezocone penetrometer			
MCPT28	2.57	67.4	2.7	PCPT10	1.79	104.4	6.0
MCPT29	2.32	92.4	4.4	PCPT11	1.74	203.5	11.7
MCPT30	2.04	77.5	4.0	PCPT12	1.99	79.7	4.3
MCPT31	2.61	104.6	4.4	15-cm^2 seismic piezocone penetrometer*			
MCPT32	2.23	96.8	4.7	SCPT15	1.87	93.3	5.6
MCPT33	2.20	85.5	4.3	SCPT20	1.58	90.2	6.2
15-cm^2 piezocone penetrometer*				SCPT25	1.70	72.2	4.6
CPT26	1.72	98.5	5.9				

* Pore water pressures were not measured during these tests.

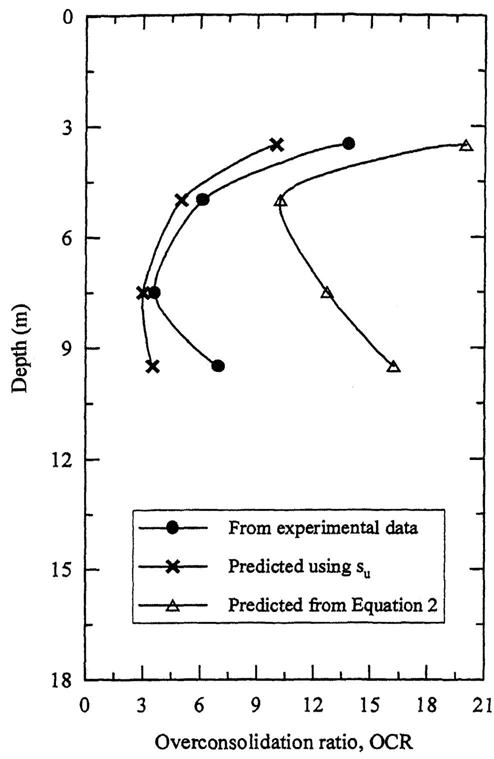

Figure 11: Comparison of predicted and measured OCR for NGES-TAMU clay site.

Conclusions

Cone penetration tests were performed at the National Geotechnical Experimentation Sites to provide the NGES users with a CPT database with cone penetrometers of different sizes (2, 10 and 15 cm^2) and functions (friction cone, piezocone, and seismic piezocone penetrometers).

Analyses of cone penetration tests conducted at the NGES at Texas A&M University–clay site was presented. Among the tests analyzed was the continuous intrusion miniature cone penetration test using the 2-cm^2 miniature cone penetrometer. The CPT and MCPT tests were used to classify the soil and identify its stratigraphy using different methods. The probabilistic region estimation and